

# Non-Equilibrium Modeling of AC Electroosmosis in Microfluidic Channels - Parametrical Studies -

M. Příbyl, P. Červenka, J. Hrdlička, and D. Šnita  
Institute of Chemical Technology, Prague, Czech Republic

**Abstract**—This Non-equilibrium mathematical model based on the balances of mass, momentum and ionic components and the Poisson equation has been developed. The model describes transport processes in the entire time and space domains including electric double layers. We assume that the system works below the electrochemical limit. The electroosmotic transport in various microfluidic channels is studied. It is considered that the channels contain a periodically repeating spatial motif. Hence the transport processes are studied in one periodic segment of the channels. Non-planar asymmetric electrodes, on which an AC electric field is imposed, are deposited on one channel wall. The model equations are solved using the finite element software COMSOL. In order to carry out the numerical simulations, a strongly anisotropic mesh of finite elements is developed. The stable periodic regimes are obtained by the time-integration of the model equations. In this work, we focus on: (i) parametric analysis of the stable periodic regimes – time-averaged characteristics (the net velocity, the current-voltage phase shift, the integral Coulomb force etc.) are computed in the parameter space, (ii) determination of regions of the parameter space, in which the net velocity attains high values, (iii) visualization of velocity fields and fields of other model variables in various phases of the AC electric signal.

**Keywords**— AC electroosmosis, microchip, mathematical modeling, non-equilibrium model, Poisson equation

## I. INTRODUCTION

Ramos *et al.* as the first studied the effects of a low amplitude AC electric field imposed on co-planar electrodes in a microchannel filled by an aqueous electrolyte [1]. They observed electrokinetic transport of a new kind above the source microelectrodes for low frequencies. Ajdari proposed a design of the AC electrokinetic micropumps based on arrays of asymmetric pairs of co-planar microelectrodes [2]. It was expected that the asymmetry of electric field will lead to a net flow of the electrolyte. His predictions were verified by several experimental and theoretical works, e.g., [3-7]. In general, the authors considered microelectrodes with the characteristic dimension from micrometers to tens of micrometers. The observed velocity of the net flow typically attained few hundreds of microns per second.

We can recognize at least three different types of the AC electroosmotic micropumps according to the microelectrode arrangement: (i) the micropumps with asymmetric co-planar electrodes, (ii) the micropumps with 3D or non-planar electrodes, and (iii) the traveling-wave electroosmotic micropumps.

Bazant *et al.* theoretically predicted that the non-planar design will increase the electrolyte net velocity up to  $\text{mm s}^{-1}$  [8, 9]. Their theory arises from the fact that the counter-rotating regions of fluid observed above the electrode arrays inhibit the net flow. Hence, the authors suggested using non-planar pumps with asymmetric raised steps. In such arrangement, the electrolyte flows in

a manner of “fluid conveyor belt” above the non-planar electrodes and the counter-rotating eddies are burrowed among the electrodes. It has been experimentally verified that the net velocity can be increased at least by one order of magnitude with respect to the pure co-planar arrangement [10, 11].

The net flow velocity in the AC micropump systems strongly depends on many parameters, e.g. [7, 11-13]: (i) the electric field parameters (amplitude, frequency, phase shift), (ii) the concentration and the composition of the used electrolyte, and (iii) geometric properties of the microfluidic system.

Mathematical models of AC electroosmosis have been developed. The computation domain is usually divided into the capacitor domains (vicinities of the polarized surfaces, i.e., the electric double layers – EDLs) and the resistor domain (electrolyte bulk). Then, boundary conditions for electric potential on the capacitor-resistor interfaces can be derived. However, these boundary conditions are valid only when a low voltage ( $\approx$  amplitude  $< 25$  mV) is applied on the microelectrodes, i.e., the linearization of the Poisson-Boltzmann equation is justified [13]. Further, the Boltzmann distribution is valid only for systems in the thermodynamic equilibrium. The AC electroosmotic systems are rarely close to the equilibrium because of the intensive convection transport at the electrode surfaces. Besides of the mathematical models relying on the capacitor-resistor slip approximation [14-16], the non-linearized Poisson-Boltzmann models [17, 18] and the non-equilibrium models [19-21] have been developed. The Poisson-Boltzmann approach allows analyzing the model equation for voltages above the linearization limit. The non-equilibrium models describe the distribution of electric potential with the use of the Poisson equation and zero (non-slip) velocity at the microelectrodes surfaces. The models based on the Poisson equation should

---

Corresponding author: Michal Příbyl  
e-mail address: pribylm@vscht.cz

Presented at the International Symposium on Electro-hydrodynamics, in March 2009

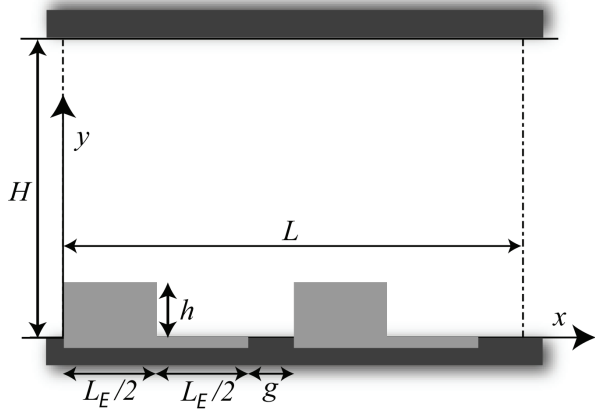


Fig. 1. Schematic configuration of a single segment of the electroosmotic micropump,  $L = 50 \mu\text{m}$ ,  $H = 80 \mu\text{m}$ ,  $L_E = 20 \mu\text{m}$ ,  $g = 5 \mu\text{m}$ . Dimensions of the system were adopted from [10, 11] in order to compare the results of the non-equilibrium model with predictions of equilibrium models and reported experiments.

satisfactorily describe the behavior of the AC electroosmotic systems with non-equilibrated dynamical EDLs even if a higher voltage is applied.

## II. NON-EQUILIBRIUM MATHEMATICAL MODEL

In this study, we consider a long microfluidic channel that contains a set of non-planar microelectrodes deposited on one wall. A two-electrode spatial motif periodically repeats along the channel, Fig. 1. So we can investigate behavior of the electroosmotic micropump in this single segment if we use periodic boundary conditions applied on the left and the right boundaries of the system. It is assumed that the width of the segment is much larger than both the segment length  $L$  and the segment height  $H$ . It means that the system is effectively two dimensional (coordinates  $x$ - $y$ ). The top boundary is considered to be a solid electric insulator.

The electric potential field  $\varphi$  satisfies the Poisson equation

$$\varepsilon \nabla^2 \varphi = -q, \quad q = F(c^+ - c^-), \quad (1)$$

where  $c^+$  and  $c^-$  are concentration of the cation and the anion, respectively, of a symmetric uni-univalent electrolyte that fills the microchannel. The symbols  $\varepsilon$ ,  $q$ , and  $F$  represent the electrolyte permittivity, the electric charge density and the Faraday constant.

In order to evaluate the distribution of electric charge, two molar balances have to be solved

$$\frac{\partial c^\pm}{\partial t} = -\nabla \cdot \left[ \mathbf{u} c^\pm - D \nabla c^\pm \mp \frac{DF}{RT} c^\pm \nabla \varphi \right], \quad (2)$$

where  $t$ ,  $\mathbf{u}$ ,  $D$ ,  $R$ , and  $T$  are time, the velocity vector, the ion diffusivity, the molar gas constant and the absolute temperature, respectively.

The velocity and pressure fields in the electrolyte are

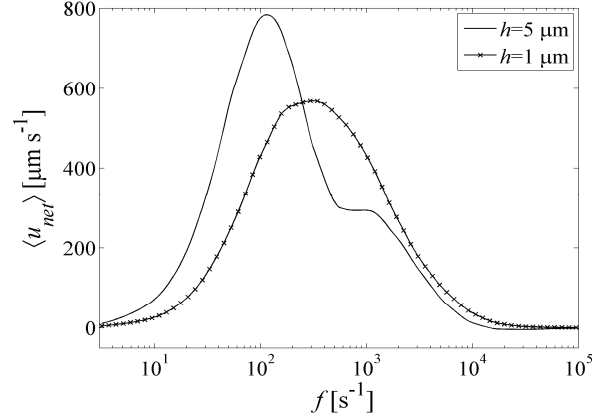


Fig. 2. Dependence of the time-averaged net velocity on the frequency of the AC electric field.

described by the Navier-Stokes equation and the continuity equation for an incompressible newtonian fluid

$$\rho \frac{\partial \mathbf{u}}{\partial t} = \eta \nabla^2 \mathbf{u} - \nabla p - q \nabla \varphi, \quad (3)$$

$$\nabla \cdot \mathbf{u} = 0. \quad (4)$$

The “steady” part of the inertial term is neglected in the Navier-Stokes equation due to a very low Reynolds number in microfluidic devices. The symbols  $\rho$ ,  $\eta$ , and  $p$  denote the electrolyte density, the electrolyte viscosity and pressure, respectively.

Non-slip boundary conditions are considered on all the solid boundaries  $\mathbf{u} = 0$ . The non-electrode solid boundaries are electric insulators  $\mathbf{n} \cdot \nabla \varphi = 0$ . All solid boundaries are impermeable for mass.

AC electric field is imposed between the electrodes

$$\varphi_L = A \sin(2\pi f t), \quad \varphi_R = 0, \quad (5)$$

where  $\varphi_L$ ,  $\varphi_R$ ,  $A$ , and  $f$  are the electric potentials imposed on the left and the right electrodes, the amplitude and the frequency of the AC electric field, respectively.

We used the following set of the model parameters:  $D = 2 \times 10^{-9} \text{ m}^2 \text{ s}^{-1}$ ,  $R = 8.314 \text{ J mol}^{-1} \text{ K}^{-1}$ ,  $F = 96485 \text{ C mol}^{-1}$ ,  $T = 310 \text{ K}$ ,  $\eta = 0.6919 \text{ mPa s}$ ,  $\rho = 993.3 \text{ kg m}^{-3}$ ,  $\varepsilon = 7.206 \times 10^{-10} \text{ F m}^{-1}$ ,  $A = 1.5 \text{ V}$ , the bulk concentration of the electrolyte  $c_0 = 3 \times 10^{-3} \text{ mol m}^{-3}$ .

Numerical analysis of the model equations was carried out in Comsol Multiphysics system. Transient simulations from the homogeneous steady state to stable periodic regimes are accomplished in the first step. The obtained stable periodic solutions were then analyzed to get the time averaged net velocity  $\langle u_{net} \rangle$ , the current-voltage phase shift  $\theta$ , the time-averaged horizontal component of the coulomb force integrated over the segment  $\langle F_x \rangle$  etc.

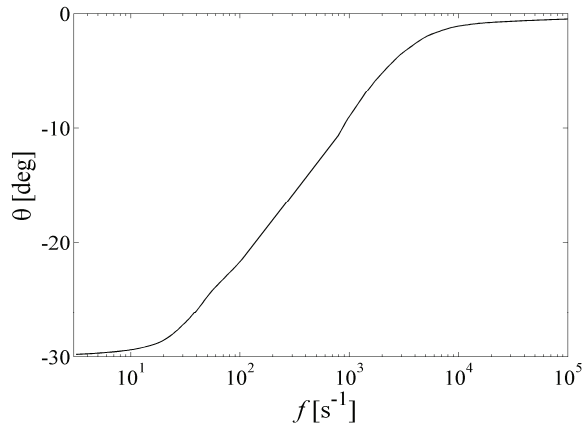


Fig. 3. Dependence of the current-voltage phase shift on the frequency of the AC electric field.

### III. RESULTS AND DISCUSSION

Frequency dependencies of selected characteristics of the AC electroosmotic pump are shown in this short study. We consider the electroosmotic system with two different electrode step heights:  $h = 5 \mu\text{m}$  and  $h = 1 \mu\text{m}$ .

The net velocity maxima are located close the frequencies that corresponds to the reciprocal charging time  $\tau_c$  of this resistor-capacitor system (the electrolyte bulk – electric double layers at the electrodes),  $f \approx \tau_c^{-1}$ , for which  $\tau_c = L\lambda_D/D$ , where  $\lambda_D$  is the Debye length, Fig. 2. The time averaged net velocity can attain almost  $1 \text{ mm s}^{-1}$ , which is a substantially bigger value than those measured for co-planar systems. The velocity dependence for  $h = 5 \mu\text{m}$  has not a single peak character. It looks more like two merged peaks. Two peak frequency characteristics were experimentally observed in [10]. The presence of the two-peak pattern probably results from the fact that there is more than one geometric length scale in this non-planar arrangement. One geometric scale is typically represented by the segment length  $L$ , another scale should be proportional to the electrode step height. Two different geometric scales necessarily lead to two different charging times and thus to the two peak frequency characteristics.

The computed current-voltage phase shifts for the both step heights were very similar. Hence, only one curve is plotted in Fig. 3. We can see that the phase shift  $\theta$  is close to the zero value for high frequencies. In such regimes, a negligible amount of electric charge is formed at the electrode surfaces and the electroosmotic pump behaves like a pure resistor. If the frequency decreases, the phase shift gradually decreases to about -30 degrees. The highest net velocities are observed just in the region of the steepest change of the phase shift. We assume that the phase shift for low velocities should be close to -90 degrees (the system behaves as a pure capacitor), i.e. the applied electric field induces a complete electrode polarization. The discrepancy between this assumption and the observed value -30 degrees is probably given

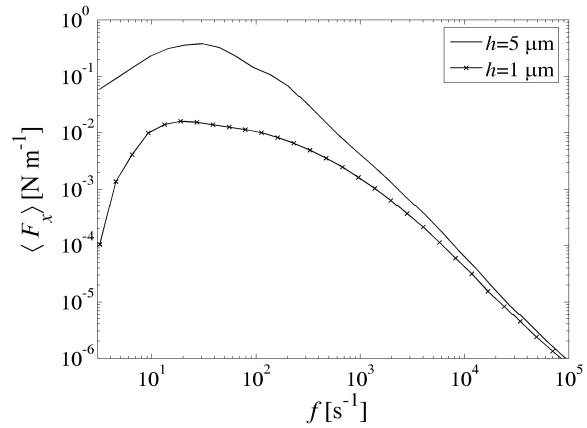


Fig. 4. Dependence of the Coulomb force integrated over the segment on the frequency of the AC electric field.

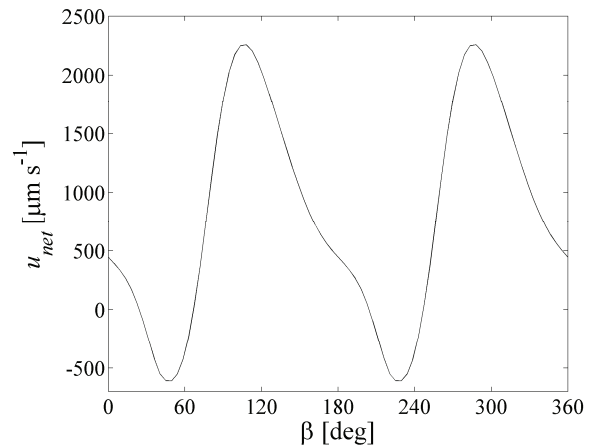


Fig. 5. Time course of the net velocity during one period of the stable periodic regime,  $f = 100 \text{ Hz}$ ,  $h = 5 \mu\text{m}$ .

either by a larger frequency extent of the system or by the existence of the complex non-planar geometry.

The dependencies of the time-averaged horizontal Coulomb force integrated over the entire segment are plotted in Fig. 4. The maxima of these dependencies are shifted to lower frequencies if compared with the maxima in Fig. 2. The horizontal Coulomb force at any point of the system is given by the product of the horizontal electric field strength and the electric charge density. If a low frequency is applied, the electrodes are fully polarized and the electric field strength is zero farther from the electrodes. The horizontal Coulomb force is quite high but localized mostly at the electrode edges. In this “capacitor” regime, the horizontal electric forces at adjacent electrode edges are fully compensated, which leads to a negligible net velocity. Further, no electric charge is formed in high frequency regimes and thus very low velocities and forces are observed. One can see that the horizontal Coulomb force is higher for the electroosmotic micropump with the electrode step height  $h = 5 \mu\text{m}$ . This fact probably corresponds to the increase of the electrode surface, which induces formation of an increasing amount of electric charge.

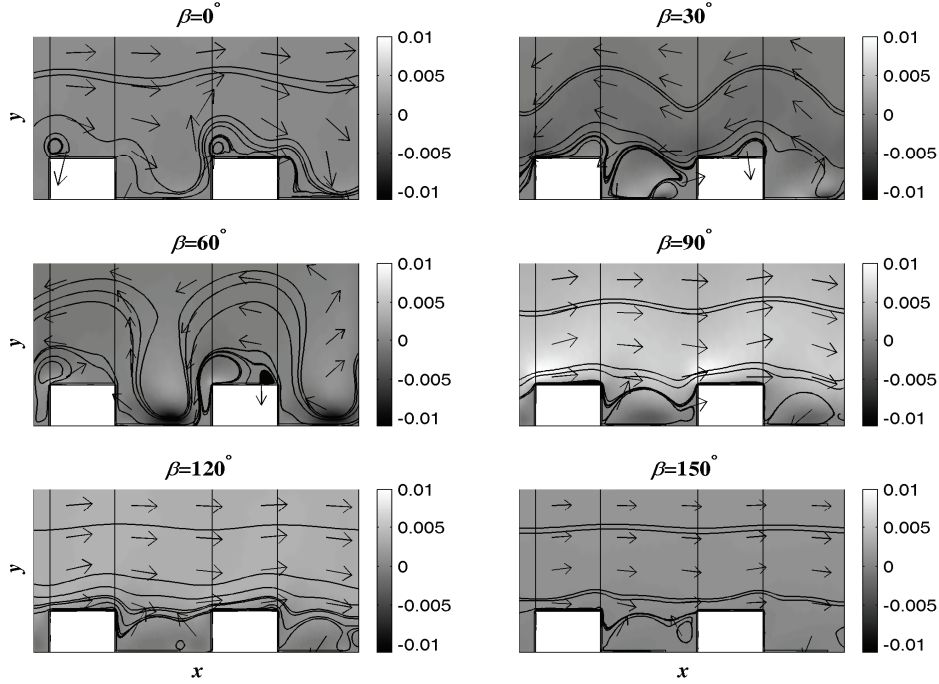


Fig. 6. The velocity field in various phases of the electric signal  $\beta$ . The color scale represents local values of the horizontal velocity in  $[\text{m s}^{-1}]$ ,  $f = 100 \text{ Hz}$ ,  $h = 5 \text{ }\mu\text{m}$ .

The time-averaged net velocity is approximately equal to  $800 \text{ }\mu\text{m s}^{-1}$  for  $f = 100 \text{ Hz}$  and  $h = 5 \text{ }\mu\text{m}$ , see Fig. 2. During one cycle of the electric signal, the velocity dramatically changes, Fig. 5. The instantaneous net velocity varies in the interval from  $-600 \text{ }\mu\text{m s}^{-1}$  to  $+2300 \text{ }\mu\text{m s}^{-1}$ . It would be useful to plot the velocity field in selected phases of the applied electric signal, Fig. 6. Due to the independency of the Coulomb force on the electric field polarity, we can study the electroosmotic flow only in one half of the electric field period.

For  $\beta = 90$  or  $120$  degrees, it is possible to see the “fluid conveyor belt” pattern of the electrolyte flow [8, 9]. The counter-rotating eddies are immersed between the electrode steps and do not substantially inhibit the net velocity. The horizontal velocity can locally attain the value  $\pm 10 \text{ mm s}^{-1}$  at electrode edges. Completely different flow pattern is obtained for  $\beta = 60$  degrees, i.e. in the phase when the net velocity is negative. Here, the electrolyte flows around the electrode steps in the opposite direction. The local horizontal Coulomb force attains the highest value at the electrode edges that are immersed between the electrode steps. So the counter-rotating eddies are dominant and the flow reversal is observed. A similar mechanism can be responsible for the flow reversal found in co-planar AC electroosmotic systems, e.g. [7, 21].

#### IV. CONCLUSION

We developed a non-equilibrium mathematical

model of the AC electroosmosis in microfluidic systems. The model was tested on a particular system that contains a set of non-planar electrodes. We computed selected frequency characteristics of the proposed micropump. We were able to localize the net velocity maxima. Our findings are in qualitative agreement with the reported experimental and theoretical data [8-11]. However, there are remarkable quantitative discrepancies especially between the predictions of the equilibrium models using the capacitor-resistor boundary condition and our non-equilibrium model. The discrepancies result from the oversimplifications of the equilibrium model (the linearization of the Poisson-Boltzmann equation, the assumption of the Boltzmann distribution of the electric charge in high frequency regimes, the assumption of the one-dimensional electric double layers etc.) and also from the errors of numerical approximations (especially for the non-equilibrium model).

We believe that the developed mathematical model can be useful for analysis of electro-transport phenomena in the AC electroosmotic systems and that its predictions are more realistic than those given by the simple capacitor-resistor approaches.

#### ACKNOWLEDGMENT

The authors thank for the support by the grant of the GAAV ČR (KAN208240651), by the grant of the MŠMT ČR (MSM 6046137306), and by the grant GAČR (GD 104/08/H055).

## REFERENCES

- [1] A. Ramos, H. Morgan, N. G. Green, and A. Castellanos, "Ac electrokinetics: a review of forces in microelectrode structures," *Journal of Physics D-Applied Physics*, vol. 31, pp. 2338-2353, 1998.
- [2] A. Ajdari, "Pumping liquids using asymmetric electrode arrays," *Physical Review E*, vol. 61, pp. R45-R48, 2000.
- [3] M. Campisi, D. Accoto, and P. Dario, "ac electroosmosis in rectangular microchannels," *Journal of Chemical Physics*, vol. 123, pp. 204724, 2005.
- [4] P. Garcia-Sanchez, A. Ramos, G. Green, and H. Morgan, "Experiments on AC electrokinetic pumping of liquids using arrays of microelectrodes," *IEEE Transactions on Dielectrics and Electrical Insulation*, vol. 13, pp. 670-677, 2006.
- [5] N. G. Green, A. Ramos, A. Gonzalez, H. Morgan, and A. Castellanos, "Fluid flow induced by nonuniform ac electric fields in electrolytes on microelectrodes. III. Observation of streamlines and numerical simulation," *Physical Review E*, vol. 66, pp. 026305, 2002.
- [6] M. Mpholo, C. G. Smith, and A. B. D. Brown, "Low voltage plug flow pumping using anisotropic electrode arrays," *Sensors and Actuators B-Chemical*, vol. 92, pp. 262-268, 2003.
- [7] V. Studer, A. Pepin, Y. Chen, and A. Ajdari, "An integrated AC electrokinetic pump in a microfluidic loop for fast and tunable flow control," *Analyst*, vol. 129, pp. 944-949, 2004.
- [8] M. Z. Bazant and Y. X. Ben, "Theoretical prediction of fast 3D AC electro-osmotic pumps," *Lab on a Chip*, vol. 6, pp. 1455-1461, 2006.
- [9] D. Burch and M. Z. Bazant, "Design principle for improved three-dimensional ac electro-osmotic pumps," *Physical Review E*, vol. 77, pp. 055303, 2008.
- [10] J. P. Urbanski, T. Thorsen, J. A. Levitan, and M. Z. Bazant, "Fast AC electro-osmotic micropumps with nonplanar electrodes," *Applied Physics Letters*, vol. 89, pp. 143508, 2006.
- [11] J. P. Urbanski, J. A. Levitan, D. N. Burch, T. Thorsen, and M. Z. Bazant, "The effect of step height on the performance of three-dimensional ac electro-osmotic microfluidic pumps," *Journal of Colloid and Interface Science*, vol. 309, pp. 332-341, 2007.
- [12] B. P. Cahill, L. J. Heyderman, J. Gobrecht, and A. Stemmer, "Electro-osmotic streaming on application of traveling-wave electric fields," *Physical Review E*, vol. 70, pp. 036305, 2004.
- [13] T. M. Squires and M. Z. Bazant, "Induced-charge electro-osmosis," *Journal of Fluid Mechanics*, vol. 509, pp. 217-252, 2004.
- [14] B. J. Kim, S. Y. Yoon, H. J. Sung, and C. G. Smith, "Simultaneous mixing and pumping using asymmetric microelectrodes," *Journal of Applied Physics*, vol. 102, pp. 074513, 2007.
- [15] N. Loucaides, A. Ramos, and G. E. Georghiou, "Novel systems for configurable AC electroosmotic pumping," *Microfluidics and Nanofluidics*, vol. 3, pp. 709-714, 2007.
- [16] L. H. Olesen, H. Bruus, and A. Ajdari, "ac electrokinetic micropumps: The effect of geometrical confinement, Faradaic current injection, and nonlinear surface capacitance," *Physical Review E*, vol. 73, pp. 056313, 2006.
- [17] T. Khan and P. M. Reppert, "A finite element formulation of frequency-dependent electro-osmosis," *Journal of Colloid and Interface Science*, vol. 290, pp. 574-581, 2005.
- [18] X. M. Wang and J. K. Wu, "Flow behavior of periodical electroosmosis in microchannel for biochips," *Journal of Colloid and Interface Science*, vol. 293, pp. 483-488, 2006.
- [19] N. A. Mortensen, L. H. Olesen, L. Belmon, and H. Bruus, "Electrohydrodynamics of binary electrolytes driven by modulated surface potentials," *Physical Review E*, vol. 71, pp. 056306, 2005.
- [20] M. Pribyl, D. Snita, and M. Marek, Multiphysical Modeling of DC and AC Electroosmosis in Micro- and Nanosystems, in *Recent Advances in Modelling and Simulation*, G. Petrone and G. Cammarata, Editors. 2008, I-Tech Education and Publishing: Vienna. pp. 501-522.
- [21] P. Cervenka, M. Pribyl, and D. Snita, "AC Micropumps – Numerical study on AC electroosmosis in microfluidic channels," *Microelectronic engineering*, vol. 86, pp. 1333-1336, 2009.